Emission spectroscopy of a pulsed helium-discharge plasma: Transition from the ionizing phase to the recombining phase

A. Hirabayashi, Y. Nambu, M. Hasuo, and T. Fujimoto

Department of Engineering Science, Kyoto University, Kyoto 606, Japan

(Received 6 February 1987)

A pulsed helium-discharge plasma was found to have two peaks in the temporal development of its emission line intensities. At these peaks the population densities of the $n\,^3D$ state ($n = 3, 4, \ldots$) were measured. For the first peak, the populations were found to be proportional to n^{-6}, while the second peak showed an $\exp[-E(n)/kT_e]$ dependence. These distributions are identified with plasma in its ionizing and recombining phases, respectively. On the basis of a collisional-radiative model calculation, the transition from the ionizing phase to the recombining phase is demonstrated. This report is the first experimental demonstration of the n^{-6} distribution in the ionizing phase for conditions when the conventional criterion would indicate thermal populations. It is suggested that the apparent decrease in the emission line intensities of high-n members of series lines, or "the transparency window" that is observed in dense plasmas, may be attributed to this characteristic of ionizing plasma.

I. INTRODUCTION

Emission properties of a plasma are determined from the population density distribution over the excited states (including continuum states) of atoms and ions in the plasma. These populations are determined as a result of various atomic processes (electron collisions and radiative transitions) taking place in the plasma, and their dependence on the plasma parameters are complicated. According to the collisional-radiative model (CR model),[1,2] however, the population density $N(n)$ of level n is simply given as a sum of the two terms, i.e., the one proportional to the ion density N_z in the next ionized stage z and another proportional to the ground-state atom or ion density $N(1)$ of this ionization stage.

$$N(n) = r_0(n)Z(n)N_z n_e + r_1(n)[Z(n)/Z(1)]N(1)$$
$$\equiv N_0(n) + N_1(n) , \tag{1}$$

where n_e is the electron density and the Saha-Boltzmann coefficient is

$$Z(n) = \frac{g(n)}{2g_z}\left[\frac{h^2}{2\pi m k T_e}\right]^{3/2} \exp\left[-\frac{E(n)}{kT_e}\right] . \tag{2}$$

Here, $g(n)$ and g_z are the statistical weights of level n and ion z, respectively, m is the electron mass, and $E(n)$ (<0) is the eigenenergy of the level.

The overall effect of the atomic processes in the plasma is represented by $r_0(n)$ and $r_1(n)$, the population coefficients, and therefore they are functions of n_e and T_e (electron temperature). The magnitude of these coefficients, which is smaller than 1 except under very special conditions, is a measure of departure of $N_0(n)$ and $N_1(n)$ from their thermodynamic equilibrium values, i.e., $r_0(n) = 1$ gives the Saha-Boltzmann [local thermodynamic equilibrium (LTE)] population with

respect to N_z and $r_1(n) = 1$ gives the Boltzmann population with respect to $N(1)$. From now on we consider the hydrogenic atom or ion for the purpose of illustration, and n in Eqs. (1) and (2) is understood to denote the principal quantum number of the level.

In many actual situations, one of the two terms in the right-hand side of Eq. (1) is dominant.[2] In situations we call the recombining phase $N_0(n)$ always dominates over $N_1(n)$. In the ionizing-phase plasma this relation is reversed. The recombining phase is realized, for example, in an afterglow plasma, and highly ionized impurity ions in the outer regions of tokamak plasmas are another example of the recombining plasma. Examples of the ionizing phase are the positive-column plasma and hydrogen and low-ionized-stage ions in tokamak plasmas. The general characteristics of the populations in both the phases are discussed in detail in Ref. 2. For example, in the recombining phase, the population densities of levels higher than Griem's[3] critical level are described by the Saha-Boltzmann equation. In the ionizing phase, on the other hand, population densities in the same levels are proportional to n^{-6}. This characteristic is the result of the multistep ladderlike excitation-ionization mechanism of electrons through the excited levels; the excitation rate for $n \rightarrow (n+1)$ is approximately proportional to n^4, and therefore $N_1(n)$ is proportional to n^{-4}, or $N_1(n)/g(n) \propto n^{-6}$. For further details the readers are referred to Ref. 2. The experimental verification of this latter population has been made only on neutral argon in an argon positive-column plasma.[2,4] Since the energy-level structure of argon is complicated and far from that of hydrogen, for which the ladderlike mechanism has originally been proposed, this observation may be claimed not to be a definite proof of the n^{-6} distribution.

One of the motives for the present study is related to the recent proposals made by one of the present authors. These proposals are concerned with excitation and deexcitation of ions in dense plasma. The first is[5] that the

conventional excitation and deexcitation rate coefficients are enhanced owing to the effect of plasma electrons on the population of doubly excited states. Dielectronic capture of an electron by an ion into a doubly excited state followed by the ladderlike excitation "ionization" enhances substantially the excitation. Autoionization of the doubly excited ion in LTE with respect to the singly excited state enhances the deexcitation from this state. The second proposal is[6] that a similar ladderlike process gives rise to an effective decrease and disappearance of the resonance contribution to the excitation cross section which is relevant to an isolated ion. In these processes the multistep ladderlike excitation-ionization mechanism plays an essential role, and an experimental verification of the establishment of this mechanism, even if it were for singly excited states of a neutral atom, would render a firm support to these proposals.

Another motive is related to the emission characteristic of dense plasma which has received much attention recently. Weisheit and Shore[7] proposed the "transparency window" in the higher member of Lyman lines of neutral hydrogen and an observation of the transparency window has been reported on mercury.[8] Höhne and Zimmermann[9] claim that the "window" is the result of a numerical artifact in the calculation of Ref. 7. The present authors feel that this problem should also be reviewed in the context of the different characteristics of the ionizing and recombining plasmas. In this paper, we report an observation of the characteristic populations in a pulsed discharge plasma in relation to the ionization imbalance of the plasma, or the ionizing and recombining phases of plasma.

II. EXPERIMENTAL SETUP

The discharge tube and the detection system were almost the same as that described in Ref. 10. A brief account is given below. The Pyrex discharge tube had an inner diameter of 5 mm and a length of 3 cm. The base pressure was 3.5×10^{-7} torr before high-purity helium was introduced. The current source was a 0.05-μF capacitor charged to 5 kV. The pulsed discharge at 10 pulses per second was run in 2 torr of helium. The discharge current was measured by a voltage drop over a shunt resistor (1 Ω). The emission was observed along the direction perpendicular to the tube axis through a monochromator-photomultiplier system. The monochromator ($f/5$) had a focal length of 250 mm and a linear reciprocal dispersion of 3.4 nm/mm. The entrance and exit slits of monochromator had widths of 70 μm and heights of 10 mm. The output of the photomultiplier (R928) was fed to a boxcar averager (PAR 162 and 164) with a gate width of 0.5 μs. The output of the boxcar averager was recorded on an X-Y recorder in the case of the temporal development or on a chart recorder in the case of the intensity spectrum at a particular time. The spectral sensitivity of the detection system had been calibrated absolutely by the in situ calibration method developed in Ref. 10: By applying the laser-induced-fluorescence spectroscopy to the positive-column plasma and employing the saturation characteristics · of the laser-produced population, we have calibrated our sys-

tem. This in situ method, in combination with the relative spectral sensitivity as determined by using a standard lamp, gives a result which is highly reliable with a small uncertainty, 10% in our case. Another advantage of this method is that the procedure includes in the sensitivity the effect of transmission and reflection by the discharge tube wall.

III. RESULT AND DISCUSSION

A. Ionizing phase and recombining phase

Figure 1(a) shows the temporal development of the discharge current: 170 A maximum and 2 μs duration. Figure 1(b) shows the temporal development of the observed emission intensity of the 587.6-nm ($2\,^3P-3\,^3D$) line taken as an example. This temporal development is divided into two parts: the first ($0 < t < 2\,\mu$s) part is obtained during the period of the discharge current. The second part ($t \geq 3\,\mu$s) starts immediately after the end of the discharge current, reaches a maximum, and then decreases slowly. Between these parts, the emission almost disappears. These characteristics were common to the emission intensities of other neutral lines, although relative intensities at the two peaks are different for different lines (see Fig. 3 later). At the first and second peaks, indicated by the arrows in Fig. 1(b), we obtained the spectrum of the $2\,^3P-n\,^3D$ ($n = 3,4,\ldots$) series lines. An example of the spectrum at the second peak is shown in Fig. 2. From the measured area under each spectral line, the population densities of the $n\,^3D$ states are obtained. The background due to the $2\,^1P-\kappa\,^1D$ continuum is taken into account as described later. The effect of radiation trapping is corrected for as follows. A concave mirror was placed at the side opposite to the monochromator, and we measured the emission intensities of the 587.6-nm ($2\,^3P - 3\,^3D$) line with and without the mirror. From the comparison, the line absorption A_L,[11] which is a measure of the optical thickness of the line, was obtained. At the first and second peaks A_L was
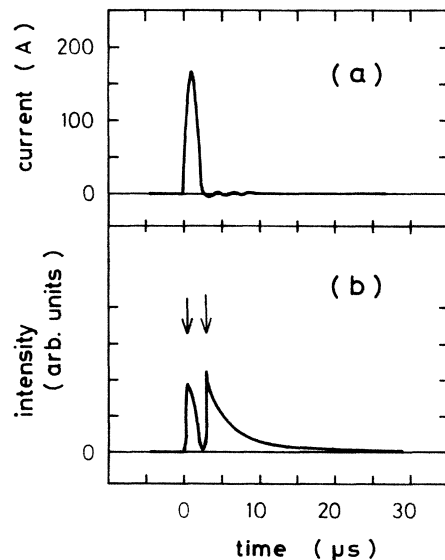

FIG. 1. Temporal development of (a) the discharge current and (b) the emission intensity of the 587.6-nm line ($2\,^3P-3\,^3D$).

0.57 and 0.46, respectively. Since the Stark widths of the spectral lines originating from the low-n states are in the present experiment much smaller than the Doppler width,[12] these lines are assumed to have the Doppler profile. By using the known oscillator strengths of the series lines, we correct the measured line intensities for the opacity effect by following the procedure described in Ref. 13. Figure 3 shows the population densities of the $n\,^3D$ states as a function of the principal quantum number in a log-log plot. For the two peaks of the emission, the population density distribution over the excited states show an obvious difference. We also measured the $2\,^1P-n\,^1D$ series lines; the intensities were lower than the triplet lines by as much as an order, but they showed the similar characteristics to the triplet lines.

It is known that any plasma may be classified into ionizing-phase, recombining-phase, or equilibrium-phase plasmas.[2] At the first peak ($t=0.5$ μs), the present result shows the n^{-6} dependence which is expected for high-density and high-temperature ionizing-phase plasma. At the second peak ($t=3$ μs), the population density tends to a finite value with increasing n. Figure 4 shows another plot of population density at the second peak: the Boltzmann plot. This shows that the population densities are well approximated by the Saha-Boltzmann equation, Eq. (2). This is expected for recombining-phase plasma. Thus, it is confirmed that the typical ionizing and recombining phases are realized in this pulsed discharge.

For the second peak, as shown in Fig. 3, the population densities of the high-n states are much higher than those for the first peak. Figure 2 shows the spectrum at the second peak (recombining phase) near the series limit of the $2\,^3P-n\,^3D$ lines. The spectral widths of the lines of $n=9,10,11,\ldots$ are so broad that the lines merge with their neighbors, resulting in a continuumlike spectrum. This leads smoothly into the true free-bound continuum. The population densities of the continuum states having positive energies are obtained from the continuum intensities through the recombination cross
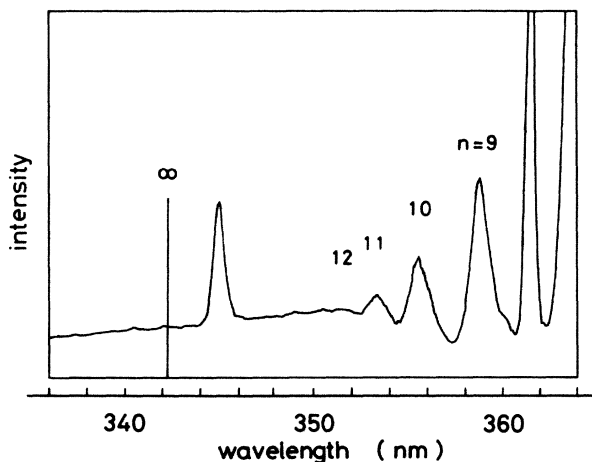

FIG. 3. Population densities of the helium $n\,^3D$ levels as a function of n. Experimental results ($\bigcirc$) are obtained in (a) the first peak and (b) the second peak. ($+$) represents the results of the collisional-radiative calculation under the condition of $N(1\,^1S)=6\times10^{22}$ m^{-3}. From the fitting, n_e and T_e are obtained, respectively, as 1.0×10^{20} m^{-3} and 4.5×10^4 K for the first peak and 1.25×10^{21} m^{-3} and 5.1×10^3 K for the second peak.

section and the state density

$$g_F = \frac{\sqrt{2}}{\pi^2 n_e}\left[\frac{m\mathcal{R}}{\hbar^2}\right]^{3/2}\left[\frac{E}{\mathcal{R}}\right]^{1/2} \quad (\mathrm{Ry}^{-1}), \qquad (3)$$

FIG. 2. Spectrum near the series limit of the $2\,^3P-n\,^3D$ transitions. The $2\,^1S-5\,^1P$ and $2\,^1S-6\,^1P$ transitions are included at $\lambda=361.4$ and 344.8 nm, respectively. The spectral sensitivity of the detector system has not been corrected for.
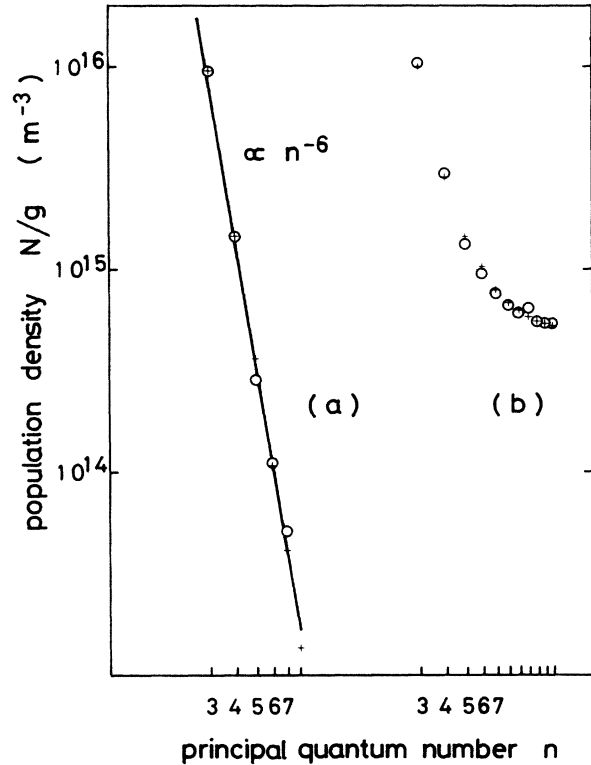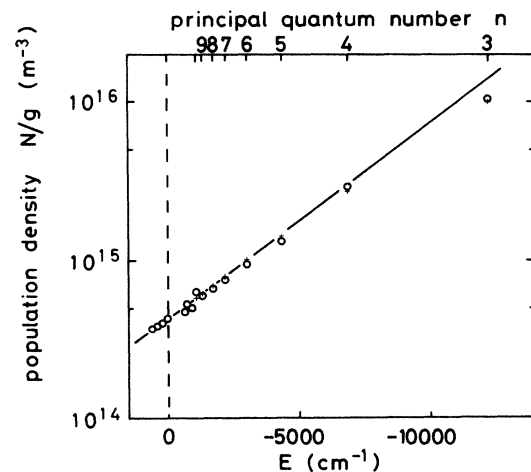

FIG. 4. Boltzmann plot of the $n\,^3D$-level populations, which is the same as given in Fig. 3(b). The solid line shows the Saha-Boltzmann populations corresponding to $n_e=1.25\times10^{21}$ m^{-3} and $T_e=5.1\times10^3$ K.

where E is the energy and $\mathcal{R}=13.6$ eV. The derivation of g_F is given in the Appendix. The recombination cross section σ_{cn} is obtained from the photoionization cross section σ_{nc} through the Milne formula,[14] where $\sigma_{nc}=8.067\times10^{-22}df/dE$ (m^2). (df/dE is the oscillator strength per unit energy interval.) For the bound-bound transitions, we have $df/dE = n^3 f(2\,^3P-n\,^3D)/2$, where $f(2\,^3P-n\,^3D)$ is taken from the calculation by Green et al.[15] For the bound-free transitions, the values of df/dE calculated by Jacobs[16] are used. As shown in Fig. 5, the values of df/dE for bound-bound and bound-free transitions are connected by a smooth curve as a function of the photon energy of the transition. In obtaining the population densities in Fig. 4 from Fig. 2 ($E\lesssim0$), the background due to the $2\,^1P-\kappa\,^1D$ continuum intensity has been taken into account as follows: For the $2\,^1P-n\,^1D$, $-\kappa\,^1D$ transitions, the values of df/dE are also shown in Fig. 5. From this figure and the Boltzmann factor $\exp(-\Delta E/kT_e)$, we find that the contribution from the $2\,^1P-\kappa^1D$ continuum is about 11% of the intensity of the continuumlike spectrum in Fig. 2. This is found to be consistent with the observed intensity of the $2\,^1P-n\,^1D$ series lines which have the series limit at 368.1 nm.

B. Electron temperature and density

In Fig. 3 we show the absolute population densities. For the two peaks of the emission radiation, the results of the CR model calculation[17] are fitted to the experimental r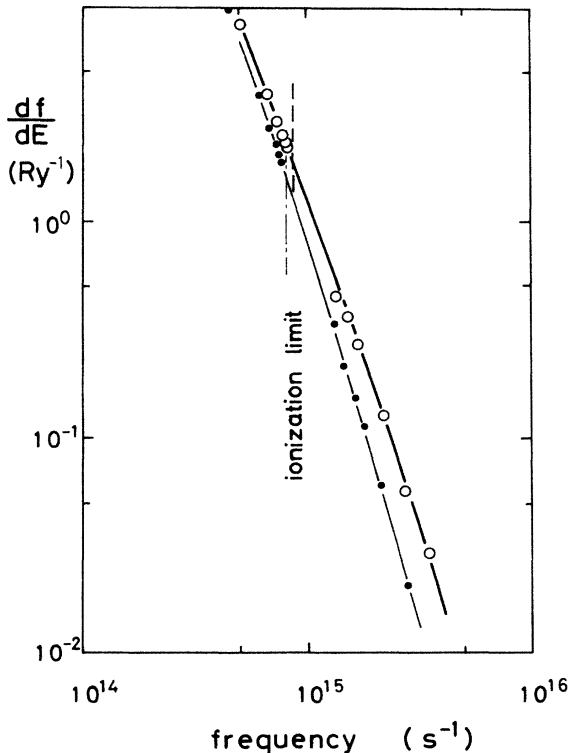esults by adjusting n_e and T_e. [The ground-state population density $N(1\,^1S)$ is assumed to be 6×10^{22} m^{-3}.] The results of the fitting are shown in Fig. 3; we obtain $n_e=1.0\times10^{20}$ m^{-3} with $T_e=4.5\times10^4$ K for the first peak (ionizing phase), and $n_e=1.25\times10^{21}$ m^{-3} with $T_e=5.1\times10^3$ K for the second peak (recombining phase).[18]

Reference 2 gives validity criteria for various approximations to hold. Griem's boundary level for the first peak is $n_G=2.1$, and $T_e=4.5\times10^4$ K is well within the high-temperature range. Thus since this plasma is in the ionizing phase, level populations with $n\gg2$ are expected to be determined by ladderlike excitation-ionization resulting in the n^{-6} distribution,[2] and consistent with our observation. For the second peak, $n_G=1.6$ and Byron's critical level is $n_B=3.2$. Thus, levels with $n\gg3$ are expected to be in partial LTE, i.e., their population densities are described by the Saha-Boltzmann equation [$r_0=1$ and $r_1=0$ in Eq. (1)]. In Fig. 4, the solid line corresponds to Saha-Boltzmann populations.

C. Transition from the ionizing phase to the recombining phase

Figure 6 shows the calculated population densities $N_0(3\,^3D)$ and $N_1(3\,^3D)$ as a function of electron temperature. This is the result of a CR model calculation for conditions where $n_e=10^{21}$ m^{-3} and $N(1\,^1S)=6\times10^{22}$ m^{-3}. In Eq. (1), we see that $N_0(3\,^3D)$ is approximately proportional to n_e^2 and that $N_1(3\,^3D)$ has a weak dependence on n_e, if $N(1\,^1S)$ is fixed. By using Fig. 6, we can
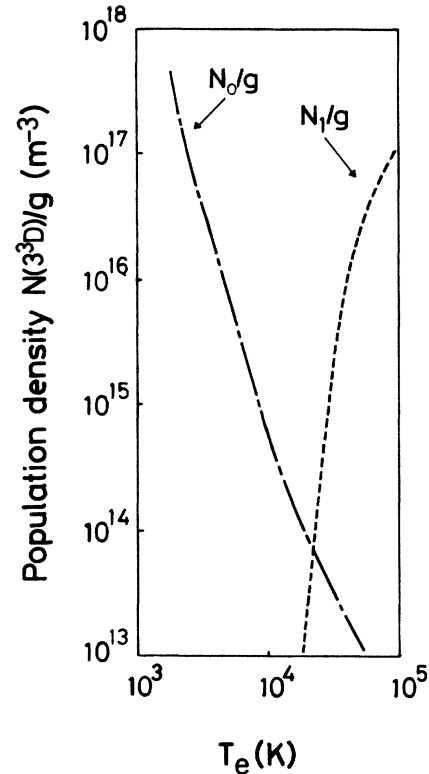

FIG. 5. df/dE as a function of the transition frequency. ($\bigcirc$), the $2\,^3P-n\,^3D$, $-\kappa\,^3D$ transitions and ($\bullet$), the $2\,^1P-n\,^1D$, $-\kappa\,^1D$ transitions.

FIG. 6. $N_0(3\,^3D)$ and $N_1(3\,^1D)$ calculated by the collisional-radiative model for conditions of $n_e=10^{21}$ m^{-3} and $N(1\,^1S)=6\times10^{22}$ m^{-3}; the actual population is given as $N(3\,^3D)=N_0(3\,^3D)+N_1(3\,^3D)$.

interpret the temporal development of the emission intensity or the peaks and the valley between them as shown in Fig. 1(b): During the period of discharge current, the electron temperature is high and $N_0 \ll N_1$; the excited states are populated mainly by electron collisions from the low-lying state atoms (ladderlike excitation), resulting in the n^{-6} distribution. When the discharge current vanishes, the electron temperature rapidly decreases and N_1 also decreases. When $N_0 = N_1$, the population density $N(3\,{}^3D)$ reaches a minimum and a transition from the ionizing to the recombining phase occurs. With a further decrease in electron temperature, the recombination of low-energy electrons with ions dominates $(N_0 \gg N_1)$, and strong emission is observed. In Fig. 6, the population density for $T_e = 2.2 \times 10^4$ K is smaller, by about two orders of magnitude, than those at $T_e = 4 \times 10^4$ K or 5×10^3 K, which show agreement with the results obtained in Sec. III A. From the above, we conclude that the phase of the present plasma changes in the valley between the two intensity peaks [at $t = 2.5$ μs in Fig. 1(b)].

The fact that the electron density at the first peak is an order lower than at the second peak is interpreted as follows: The first peak corresponds to the period during the course of ionization, while the second peak corresponds to the time just after the termination of the ionization of the plasma.

As has been shown, the line intensities, or the excited-state populations, are determined by the electron temperature and density; roughly speaking, the former determines the ionization imbalance, i.e., whether the plasma is ionizing or recombining, and the latter determines the absolute magnitude of the population. If the current pulse were cut more sharply than the present case, we would expect to have a plasma with higher electron density with the same low temperature. We would then have stronger emissions for the second peak which stems from the first term of Eq. (1). By reducing the reactance of our circuit we actually reduced the fall time of the current. We then observed at the beginning of afterglow a sharp peak which is about an order stronger than that in Fig. 1(a).

D. The energy-level structure

The n^{-6} distribution in the ionizing-phase plasma is the result of the ladderlike excitation mechanism in the Rydberg-series levels. In this context, neutral argon, only with which this distribution has so far been observed,[2,4] is less adequate, because it has doublet ionization limits and has a complicated fine structure. In the case of helium, on the other hand, the level structure is simple, and it is easy to observe the series lines, e.g., $2\,{}^3P - n\,{}^3D$ in the present study. Furthermore, we can make a reliable collisional-radiative calculation for helium.[17]

The fact that n^{*-6} distribution is valid even for argon (here n^* denotes the effective principal quantum number) appears to suggest that the ladderlike excitation-ionization mechanism is common to other various atoms and ions having a complicated level structure than hydrogen or helium. The above argument may also apply

to doubly excited states which have been discussed in Refs. 5 and 6. In ionizing plasma the population of a doubly excited state—for example, heliumlike $2pnl$—is subject to the ladderlike excitation-ionization, resulting in hydrogenlike $2p$. The initial population may be the result of dielectronic capture of hydrogenlike $1s$ in the present example. Thus, effective excitation of $1s \rightarrow 2p$ has taken place. The finding of the present study appears to render a support to the proposals in Refs. 5 and 6.

E. The transparency window

Figures 3 and 6 show that the line series emitted during the ionizing and recombining phases have quite different spectral characteristics. The arguments concerning the existence of the transparency window so far have implicitly assumed the equilibrium plasma, the spectral characteristics of which are essentially the same as the recombining plasma in the present example. If the series of lines were observed from an ionizing plasma and analyzed assuming an equilibrium plasma, then one would be led to the conclusion that the higher-n lines are much weaker than expected. Thus, the present study strongly suggests that in the experiment concerning the transparency window, care should be taken to determine the correct state of ionization balance of the plasma, i.e., whether the plasma is ionizing, recombining, or equilibrium.

APPENDIX: STATE DENSITY

First, we consider the state density of free electrons having a momentum of $p = \sqrt{2mE}$ $(E > 0)$. The number of states is

$$g = \frac{\Delta p_x \Delta q_x}{h} \frac{\Delta p_y \Delta q_y}{h} \frac{\Delta p_z \Delta q_z}{h}$$

$$= \frac{4\pi p^2 \Delta p \, \Delta V}{h^3} . \tag{A1}$$

Each particle has a volume of $\Delta V = n_e^{-1}$. The state density of free electrons is $2g$; the factor 2 comes from the two directions of spin. Then we obtain

$$g_F = \frac{\sqrt{2}}{\pi^2 n_e} \left[\frac{m\mathcal{R}}{\hbar^2} \right]^{3/2} \left[\frac{E}{\mathcal{R}} \right]^{1/2} \quad (\text{Ry}^{-1}) . \tag{A2}$$

Second, we consider electrons in bound states $(E < 0)$ with a principal quantum number n. The statistical weight of $2n^2$ and the energy separation between the adjacent states of $2\,\mathcal{R}/n^3$ yield the state density,

$$g_B = \left[-\frac{\mathcal{R}}{E} \right]^{5/2} \quad (\text{Ry}^{-1}) . \tag{A3}$$

[1]D. R. Bates, A. E. Kingston, and R. W. P. McWhirter, Proc. R. Soc. London 267, 297 (1962); D. R. Bates and A. E. Kingston, Planet. Space. Sci. 11, 1 (1963); R. W. P. McWhirter and A. G. Hearn, Proc. Phys. Soc. London 82, 641 (1963).

[2]T. Fujimoto, J. Phys. Soc. Jpn. 47, 265 (1979); 47, 273 (1979); 49, 1561 (1980); 49, 1569 (1980); 54, 2905 (1985).

[3]H. R. Griem, Phys. Rev. 131, 1170 (1963).

[4]K. Tachibana and K. Fukuda, Jpn. J. Appl. Phys. 12, 895 (1973).

[5]T. Fujimoto and T. Kato, Phys. Rev. Lett. 48, 1022 (1982); Phys. Rev. A 32, 1663 (1985).

[6]T. Fujimoto and T. Kato, Phys. Rev. A 35, 3024 (1987).

[7]J. C. Weisheit and B. W. Shore, Astrophys. J. 194, 519 (1974); G. A. Kobzev, Yu. K. Kurilenkov, and G. É. Norman, Teplofiz. Vys. Temp. 15, 193 (1977) [High Temp. (USSR) 15, 163 (1977)].

[8]Yu. K. Kurilenkov and P. V. Minaev, Zh. Eksp. Teor. Fiz. 74, 563 (1978) [Sov. Phys.—JETP 47, 295 (1978)].

[9]F. E. Höhne and R. Zimmermann, J. Phys. B 15, 2551 (1982).

[10]A. Hirabayashi, S. Okuda, Y. Nambu, and T. Fujimoto, Appl. Spectrosc. 40, 841 (1986).

[11]A. C. G. Mitchell and M. W. Zemansky, Resonance Radiation and Excited Atoms (Cambridge University Press, Cambridge, England, 1971).

[12]H. R. Griem, Spectral Line Broadening by Plasmas (Academic, New York, 1974).

[13]T. Fujimoto, C. Goto, and K. Fukuda, Phys. Scr. 26, 443 (1982).

[14]J. Cooper, Rep. Progr. Phys. 29, 35 (1966).

[15]L. C. Green, N. C. Johnson, and E. K. Kolchin, Astrophys. J. 144, 369 (1966).

[16]V. L. Jacobs, Phys. Rev. A 9, 1938 (1974).

[17]T. Fujimoto, J. Quant. Spectrosc. Radiat. Transfer 21, 439 (1979).

[18]For the second peak, we have applied Vidal's method and obtained $n_e = 1.4 \times 10^{21}$ m^{-3} [C. R. Vidal, J. Quant. Spectrosc. Radiat. Transfer 6, 461 (1966)].